Journal of Applied Polymer Science

Mechanical and Thermal Properties of Hierarchical Composites Enhanced by Pristine Graphene and Graphene Oxide Nanoinclusions

B. Zhang,[1] R. Asmatulu,[1] S. A. Soltani,[2] L. N. Le,[1] S. S. A. Kumar[1]

[1]Department of Mechanical Engineering, Wichita State University, 1845 Fairmount, Wichita, Kansas 67260-0133

[2]Department of Aerospace Engineering, Wichita State University, 1845 Fairmount, Wichita, Kansas 67260-0133

Correspondence to: R. Asmatulu (E-mail: ramazan.asmatulu@wichita.edu)

ABSTRACT: Epoxy resin nanocomposites incorporated with 0.5, 1, 2, and 4 wt % pristine graphene and modified graphene oxide (GO) nanoflakes were produced and used to fabricate carbon fiber-reinforced and glass fiber-reinforced composite panels via vacuum-assisted resin transfer molding process. Mechanical and thermal properties of the composite panels—called hierarchical graphene composites—were determined according to ASTM standards. It was observed that the studied properties were improved consistently by increasing the amount of nanoinclusions. Particularly, in the presence of 4 wt % GO in the resin, tensile modulus, compressive strength, and flexural modulus of carbon fiber (glass fiber) composites were improved 15% (21%), 34% (84%), and 40% (68%), respectively. Likewise, with inclusion of 4 wt % pristine graphene in the resin, tensile modulus, compressive strength, and flexural modulus of carbon fiber (glass fiber) composites were improved 11% (7%), 30% (77%), and 34% (58%), respectively. Also, thermal conductivity of the carbon fiber (glass fiber) composites with 4% GO inclusion was improved 52% (89%). Similarly, thermal conductivity of the carbon fiber (glass fiber) composites with 4% pristine graphene inclusion was improved 45% (80%). The reported results indicate that both pristine graphene and modified GO nanoflakes are excellent options to enhance the mechanical and thermal properties of fiber-reinforced polymeric composites and to make them viable replacement materials for metallic parts in different industries, such as wind energy, aerospace, marine, and automotive. © 2014 Wiley Periodicals, Inc. J. Appl. Polym. Sci. **2014**, *131*, 40826.

KEYWORDS: composites; graphene and fullerenes; mechanical properties; nanotubes; thermal properties

Received 16 February 2014; accepted 6 April 2014

DOI: 10.1002/app.40826

INTRODUCTION

Fiber-reinforced polymer composites (FRPCs) are increasingly being used for structural and non-structural applications in a variety of industries, such as aerospace and automotive.[1] The superior tensile strength-to-weight and stiffness-to-weight ratios of FRPCs make them a viable replacement for metals especially for aerospace applications; however, FRPCs are more brittle than metals, and their through-the-thickness mechanical properties are much lower than their in-plane properties.[2] Moreover, FRPCs have lower electrical and thermal conductivity values compared to metals; therefore, they are more prone to electrostatic discharge-induced damages due to the lower attenuation of electromagnetic radiation,[3] and also, they exhibit inferior heat transfer and thermo-mechanical properties, which, in turn, affect their overall flammability.

Much effort has been devoted over the past few years to enhance FRPC properties by incorporating nanomaterials such as carbon nanotubes (CNTs) and carbon nanofibers (CNFs).[4–15] Fan et al.[8] studied the increase of interlaminar shear strength of a fiber-reinforced epoxy resin by adding multi-walled carbon nanotubes (MWCNTs). Short-beam shear tests and compression shear tests were conducted to characterize the effect of the MWCNTs. Results indicated that the interlaminar shear strength improved by more than 30% in the presence of MWCNTs. Mei et al.[7] added multi-scale CNTs to carbon fiber-reinforced epoxy composites and observed a high interfacial strength. Also, Bekyarova et al.[6] performed similar research but used the vacuum-assisted resin transfer molding (VARTM) process to make different nanocomposites. The authors reported that CNTs helped increase the interlaminar shear strength by 30% compared to neat epoxy resin composites. Green et al.[16] dispersed CNFs in an epoxy resin used to fabricate glass fiber-reinforced epoxy composites with vacuum-assisted resin infusion molding (VARIM). They observed a 23–26% increase in flexural strength and 25% increase in interlaminar shear strength by adding 1 wt % CNFs to the FRPC. Bortz et al.[5] reported a 35% increase in interlaminar fracture toughness of a carbon fiber-reinforced epoxy composite fabricated by the VARTM process with 1 wt % CNFs in the matrix.

Pristine graphene, a single layer of sp^2-bonded carbon atoms arranged in a two dimensional lattice, is a newly discovered

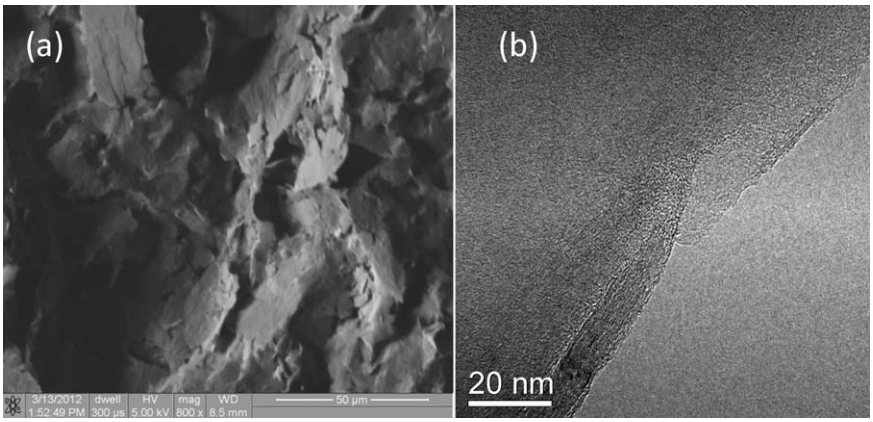

Figure 1. (a) SEM and (b) TEM images of pristine graphene nanoflakes used in the present study.

nanomaterial[17] that has been much less utilized to enhance FRPC properties despite its proven potential to increase the electrical, thermal, and mechanical properties of polymer nanocomposites.[18–20] In the majority of these studies, chemically or thermally exfoliated graphene is used and not the pristine graphene. Yavari et al.[21] reported that inclusion of 0.2 wt % of graphene into glass fiber/epoxy composites enhanced their flexural bending fatigue life up to 1200 times. Asmatulu et al.[22] improved the resistance of UV protection coatings developed for glass fiber-reinforced composites by incorporating graphene in the coating.

One of the main technical difficulties in the application of pristine graphene is its poor degree of dispersion in organic polymer matrices. As such, surface modification of pristine graphene is deemed necessary to improve its dispersion in organic polymer matrices. Oxidizing pristine graphene to obtain graphene oxide (GO) is the main surface modification method used to advance its dispersion in polymer resins. The functional groups such as hydroxyl, epoxide, carbonyl, and carboxylic acid are formed on the surface of GO, thus providing the anchoring points for nanoparticles to reinforce the composites. Once purified and dried at low temperatures, GO can be exfoliated by sonication in polar solvents to form GO sheets that exhibit improved dispensability in organic polymer resins. Zhang et al.[23] observed a 12.7% increase in the interlaminar shear strength of carbon fiber/epoxy composites after introducing 5 wt % of GO sheets into the carbon fiber sizing.

However, the effect of graphene and GO inclusion on physical and mechanical properties of FRPCs has not yet been studied thoroughly. This study reports the results of a comprehensive study on fabrication and characterization of hierarchical graphene composites consisting of carbon fiber- and glass fiber-reinforced epoxy composites enhanced with pristine graphene and GO as nanoinclusion materials in the epoxy matrix. These results indicate an increase in the thermal and mechanical properties of the FRPCs after the inclusions of pristine graphene and GO.

EXPERIMENT

Materials

Pristine graphene, with an average physical size of less than 15 μm in the x and y dimensions and 50–100 nm in the Z dimension, was purchased from Angstron Materials, Inc. (Dayton, OH). The average density of the purchased graphene in fine grayish-black powder was 2.2 g/cm^3 and contained 0.6% hydrogen, 0.5% nitrogen, and 0.8% oxygen. Figure 1 shows the scanning electron microscopy (SEM) and transmission electron microscopy (TEM) images of the pristine graphene nanoflakes.

Epon 862 resin (diglycidyl ether of bisphenol F) and Epikure curing agent W (diethyl toluene diamine) were purchased from Momentive Specialty Chemicals, Inc. (Gahanna, OH). The density and viscosity of Epon 862 at 25°C are 1.16 g/cc and 6.5–9.5 Pa.s, respectively.[24] The resin and curing agent were mixed at the recommended ratio of 100 to 27 by weight and cured at room temperature. Epon 862/Epikure W was used for the VARTM process since it offers superior physical properties, chemical resistance, and good adhesion.

Aerospace-grade plain woven (PW) carbon fiber and glass fiber plies were used as reinforcement. The carbon fiber was HexForce™ 282-PW, with a thickness of 0.26 mm and areal density of 197 g/m^2. The glass fiber was HexForce™ 7781-PW, with a thickness of 0.22 mm and areal density of 299 g/m^2.

Synthesis of Graphene Oxide

To synthesize GO, nitric acid and sulfuric acid were mixed in a (3 : 1) volume ratio to the reflux pristine graphene at a high temperature for 4 h. This was followed by the neutralization of the acidic mixture. About 4 g of GO was then mixed with the solution according to Park et al.[25] recipe and the resulting mixture was mixed and stirred with 500 mL deionized water for one day. The solution was lab-scale sonicated at 20 kHz using an FS60D sonicator (Fischer Scientific, Pittsburg, PA) for 2 h before adding 5 mL of KOH and stirring for another 2 h. Subsequently, 0.5 g of hydrazine was added to the solution and it was stirred for 6 h at 35°C. The solution was then dried to obtain the GO. Figure 2 depicts a schematic of the process of adding oxide functional groups onto the surface of graphene. The created functional group does not chemically react with epoxy resin; however, it does provide a strong polar intermolecular force between the resin and the fiber.

Dispersion of Nanoinclusions in Epoxy Resin

Pristine graphene was mixed with the epoxy resin in a beaker at the specified weight percentage before adding the curing agent.

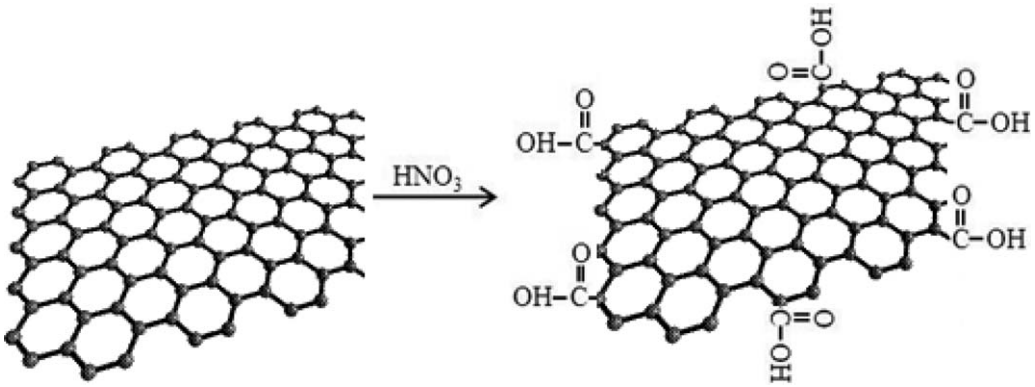

Figure 2. Schematic of graphene oxidization in concentrated acidic solution.

The mixture was mixed thoroughly using mechanical stirring for 24 h followed by 30 min of lab-scale sonication at 20 kHz using an FS60D sonicator (Fischer Scientific, Pittsburg, PA). To maintain the temperature at 25°C during the sonication process, the beaker was submerged in a water bath. The curing agent was then added to the beaker and stirred by hand using a glass rod. The resin was degasified in a vacuum chamber to remove the bubbles created during the mixing. The same method was used to mix GO nanoflakes with the resin.

Fabrication of Hierarchical Graphene Composites

A total of 18 fiber-reinforced epoxy composite panels were fabricated using the VARTM process. The resin system used for all panels was Epon 862/Epikure W. Nine panels were fabricated with eight plies of HexForce™ 282-PW carbon fiber, and nine panels were fabricated with eight plies of HexForce™ 7781-PW glass fiber. Four carbon fiber and four glass fiber panels were fabricated with the inclusion of 0.5, 1, 2, and 4 wt % of pristine graphene into the resin. Likewise, four carbon fiber and four glass fiber panels were fabricated by inclusion of 0.5, 1, 2, and 4 wt % of carboxylic acid-functionalized GO into the resin. One carbon fiber panel and one glass fiber panel were fabricated with no nanoinclusion to serve as base panels.

For the panels with the nanoinclusion, the designated resin/nanoinclusion mixture was first brush painted layer by layer on each of the eight fabric layers used for panel fabrication (Figure 3). This step was particularly important since it minimized the filtration effect in the VARTM process for mixtures containing more than 1 wt % of nanoinclusion.[26] The fabric layers were laid up in the 0 direction, and the VARTM process was carried out subsequently. The panels were cured for approximately 24–30 h at room temperature. The cured panels were machined into mechanical and thermal conductivity testing coupons.

Mechanical Characterization

A hydraulic load frame (MTS 810 Material Test System, MTS Systems Corporation, Eden Prairie, MN) was used to obtain the tensile modulus, compressive strength, and flexural modulus of the test coupons at room temperature according to ASTM D3039, ASTM D6641, and ASTM D7264 standards, respectively.

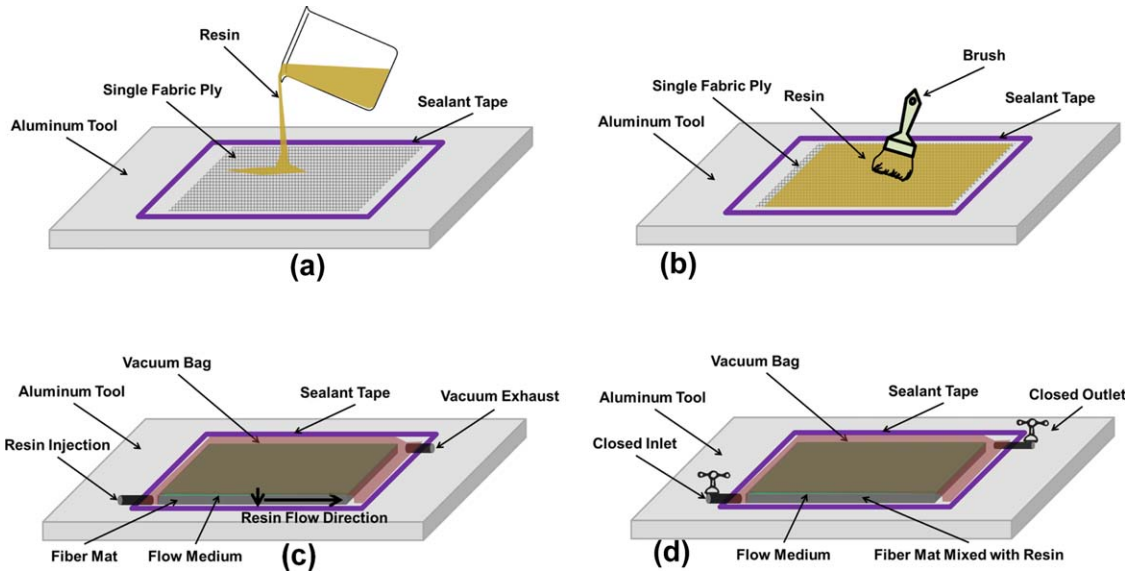

Figure 3. Panel fabrication process: (a) resin/nanoinclusion mixture poured onto first fabric layer, (b) fabric layer fully covered by resin, (c) VARTM process performed after fabric plies were laid up and vacuum bagged, (d) the panel cured at room temperature. [Color figure can be viewed in the online issue, which is available at wileyonlinelibrary.com.]

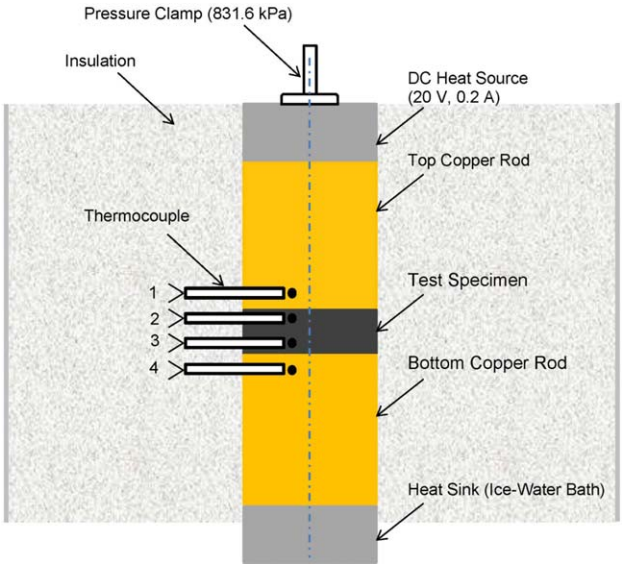

Figure 4. Schematic of thermal conductivity measurement setup. [Color figure can be viewed in the online issue, which is available at wileyonlinelibrary.com.]

Three coupons per panel were tested for each mechanical testing. The testing coupons were loaded at a constant crosshead speed of 1.3 mm/min.

Thermal Characterization

Thermal conductivity was measured per ASTM E1225. Three circular-shaped samples with a diameter of 12.8 mm and a thickness of 2.34 mm were tested from each panel. Figure 4 is a schematic of the setup used to measure thermal conductivity of the composite specimens. The setup consisted of two vertical copper rods that sandwiched a specimen with an adjustable pressure. To create temperature gradients in the rods and specimen, the top rod was connected to a heat source, and the bottom rod was connected to a heat sink. The outer surface of the copper rods and the specimen were fully insulated to ensure 1-D heat flow between the heat source and the heat sink. Four K-type thermocouples were attached to Points 1, 2, 3, and 4 to measure voltage. Voltage measurements were taken, once steady-state heat flow was achieved.

The specimen was placed between Points 2 and 3, as shown in Figure 4. A constant force was placed on top of the setup to ensure good contact between the specimen and the copper rods. The voltage difference between each two consecutive points was measured by a digital multimeter, and it was experimentally determined that 1 mV voltage difference equaled 5.6°C temperature difference.[27,28] The heat fluxes between Points 1 and 2 and also between Points 2 and 3 were calculated using the following equations, respectively:

$$q_{1-2} = K_{\text{copper}} A \frac{\Delta T_{1-2}}{\Delta x_{1-2}} \quad (1)$$

$$q_{3-4} = K_{\text{copper}} A \frac{\Delta T_{3-4}}{\Delta x_{3-4}} \quad (2)$$

where q is the heat flux between the reference points, ΔT is the temperature difference between the reference points, Δx is the distance between the reference points (5 mm for adjacent points), indices represent the reference points, A is the cross-sectional area of the copper rods, and K_{copper} is the thermal conductivity of copper. Finally, thermal conductivity of the specimen was calculated using the following equation:

$$K_S = \frac{q_{1-2} + q_{3-4}}{2} \frac{\Delta x_S}{\Delta T_{2-3} A} \quad (3)$$

where K_S is the thermal conductivity of the specimen, Δx_S is the thickness of the specimen, and A is the cross-sectional area of the test specimen, which was essentially the same as that of the copper rods. The setup was calibrated according to the procedure explained by Khan[27] using composite specimens with the known thermal conductivity values as calibration samples.

RESULTS AND DISCUSSION

Mechanical Characterization

Tables I and II give the mechanical properties of the graphene and GO hierarchical carbon and glass fiber-reinforced composites, respectively. It was observed that for all panels, the measured mechanical properties were improved consistently by increasing the weight percentage of the nanoinclusion. It is notable that the tensile modulus of the base carbon fiber reinforced panel was improved 6, 9, 13, and 15% by adding 0.5, 1, 2, and 4 wt % GO to the resin, respectively. On the other hand, inclusion of the same amounts of pristine graphene in the resin increased the tensile modulus of the base carbon fiber panel 3, 7, 8, and 11%, respectively. Likewise, 6, 8, 16, and 21% improvement in tensile modulus of the base glass fiber panel was observed by adding 0.5, 1, 2, and 4 wt % GO to the resin, respectively. Additionally, inclusion of the same amounts of pristine graphene in the resin improved tensile modulus of the base glass fiber panel about 2, 3, 4, and 7%, respectively.

As can be seen in Tables I and II, adding 0.5, 1, 2, and 4 wt % GO to the resin improved the flexural modulus of the base carbon fiber panel up to 7, 17, 31, and 40%, respectively, while inclusion of the same amounts of pristine graphene in the resin increased the flexural modulus of the base carbon fiber panel 6, 7, 27, and 34%, respectively. Tables I and II also show a significant increase in compressive strength of the specimens with the nanoflakes inclusions. It was observed that adding 0.5, 1, 2, and 4 wt % GO to the resin improved the compressive strength of the base carbon fiber panel 14, 23, 32, and 34%, respectively. Also, inclusion of the same amounts of pristine graphene in the resin increased compressive strength of the base carbon fiber panel 7, 18, 19, and 30%, respectively.

These test results indicate that the effect of nanoinclusions was more considerable on the compressive strength of the glass fiber-reinforced panel than other mechanical properties investigated in the present study. For these panels, adding 0.5, 1, 2, and 4 wt % GO to the resin increased compressive strength of the base glass fiber panel 5, 30, 61, and 84%, respectively. Likewise, adding the same amounts of pristine graphene to the resin improved the compressive strength of the base glass fiber-reinforced panel 3, 26, 58, and 77%, respectively. The increase in compressive strength for all panels with nanoinclusion could

Table I. Mechanical Properties of Carbon Fiber Composites as a Function of Pristine Graphene and Graphene Oxide Nanoinclusions

Inclusion type and weight percentage	Tensile modulus (GPa)	Increase (%)	Compressive strength (MPa)	Increase (%)	Flexural modulus (MPa)	Increase (%)
No nanoinclusion	41.50 ±1.20	-	240.99 ± 10.34	-	32.53 ± 2.12	-
0.5% Graphene	42.63 ± 1.30	2.72	257.46 ± 12.03	6.83	34.45 ± 2.45	5.90
1% Graphene	44.33 ± 1.12	6.82	285.29 ± 9.34	18.38	34.71 ± 1.23	6.70
2% Graphene	44.81 ± 1.34	7.98	287.95 ± 14.56	19.49	41.42 ± 3.45	27.33
4% Graphene	46.07 ± 0.98	11.01	312.39 ± 16.43	29.63	43.55 ± 3.21	33.88
0.5% GO	44.16 ± 1.23	6.41	273.81 ± 19.34	13.62	34.71 ± 3.56	6.70
1% GO	45.17 ± 1.43	8.84	296.40 ± 12.34	22.99	38.03 ± 2.34	16.91
2% GO	46.83 ± 1.33	12.84	317.22 ± 14.55	31.63	42.71 ± 2.01	31.29
4% GO	47.67 ± 1.20	14.87	321.78 ± 11.45	33.52	45.70 ± 2.44	40.49

Percentage increase is calculated with respect to base panel with no nanoinclusion.

be due to the decrease in shear compliance of the resin, as well as improved fiber–resin interface.

The increase in mechanical properties of fiber-reinforced composites as a result of the matrix nanomodification can be attributed to (a) enhanced interfacial bond between matrix and fibers and (b) more restricted motion of the polymer molecules. Various studies have shown that the presence of different nanoinclusions in epoxy resin can significantly improve the fiber–matrix interfacial strength.[29–31] Rahman et al.[31] reported that inclusion of 0.3 wt % CNTs in E-glass fiber/epoxy composites improved the tensile elastic modulus and strength by 18 and 20%, respectively. They also utilized fractography to demonstrate that the nanoinclusions improved the adhesion between glass fiber and matrix. The increase in tensile modulus of the composites could also indicate a more restricted motion of the polymer molecules due to the configuration of nanoinclusion particles. Since GO is dispersed better than pristine graphene in the epoxy resin, the increase in tensile modulus is more pronounced for the specimens with the GO inclusion than those with the pristine graphene inclusion for both carbon fiber- and glass fiber-reinforced panels. The configuration of nanoflakes in the resin also results in reduced deformability of the resin, which in turn, leads to an increase in the flexural modulus[32] for both carbon fiber- and glass fiber-reinforced panels.

Moreover, it was observed that the improvement of mechanical properties of hierarchical graphene composites with GO inclusion was more pronounced than those of pristine graphene inclusion. This observation is particularly important since the mechanical properties of GO are inferior to those of pristine graphene due to the disruption of the structure through oxidation as well as sp^3 bonding rather than sp^2 bonding.[33] A number of reasons were offered to explain this observation including the following: (a) GO results in more restricted motion of the polymer molecules than pristine graphene due to the difference in configuration of nanoparticles in the epoxy resin,[32] (b) GO is dispersed better than pristine graphene in the epoxy resin, and (c) the bond between GO and epoxy resin is stronger than the bond between pristine graphene and epoxy resin, which results in better adhesion of the epoxy resin enhanced with GO in the reinforcing fibers.

Table II. Mechanical Properties of Glass Fiber Composites as Function of Pristine Graphene and Graphene Oxide Nanoinclusions

Inclusion type and weight percentage	Tensile modulus (GPa)	Increase (%)	Compressive strength (MPa)	Increase (%)	Flexural modulus (MPa)	Increase (%)
No nanoinclusion	20.75 ± 1.23	-	106.66 ± 6.54	-	13.81 ± 1.23	-
0.5% Graphene	21.25 ± 1.45	2.41	109.93 ± 6.55	3.07	15.06 ± 1.45	9.05
1% Graphene	21.35 ± 1.34	2.89	134.25 ± 6.12	25.87	16.66 ± 1.64	20.64
2% Graphene	21.52 ± 1.43	3.71	168.26 ± 4.56	57.75	19.64 ± 2.54	42.22
4% Graphene	22.22 ± 1.65	7.08	188.32 ± 9.43	76.56	21.80 ± 3.65	57.86
0.5% GO	22.01 ± 1.65	6.07	112.28 ± 5.93	5.27	15.70 ± 1.21	13.69
1% GO	22.51 ± 1.34	8.48	139.00 ± 8.32	30.32	17.44 ± 1.55	26.29
2% GO	23.98 ± 1.23	15.57	171.72 ± 12.43	61.00	20.73 ± 2.01	50.11
4% GO	25.18 ± 1.76	21.35	196.22 ± 18.43	83.97	23.14 ± 2.87	67.56

Percentage increase is calculated with respect to base panel with no nanoinclusion.

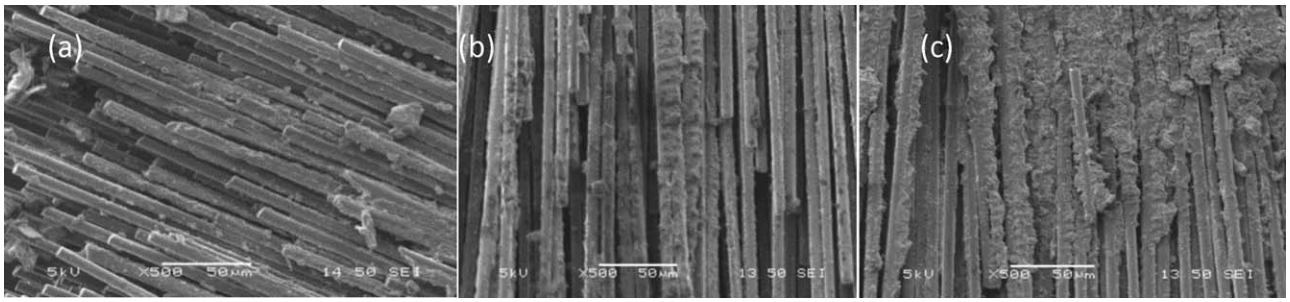

Figure 5. SEM images of tensile breakage surfaces of carbon fiber reinforced specimens: (a) base specimen with no nanoinclusion, (b) specimen with 4 wt % inclusion pristine graphene, and (c) specimen with 4 wt % inclusion GO.

To further investigate the dispersion of nanoflakes in the carbon fiber-reinforced specimens, the morphology of their tensile breakage surface were studied using SEM analysis. Figure 5(a–c) illustrates the images taken from a specimen with no nanoinclusion, a specimen with 4 wt % inclusion of pristine graphene, and a specimen with 4 wt % inclusion of GO nanoflakes, respectively. Note that in these images, only the single fiber strands, not the main woven fabrics, are depicted due to the high magnification ratio. The images show that the epoxy resin filled with GO accumulates on the surface of the carbon fibers more than the epoxy resin filled with pristine graphene. Furthermore, the epoxy resin filled with pristine graphene accumulates on the surface of the carbon fibers more than the base epoxy with no nanoinclusion. This suggests that the bonds between the nanoinclusion and the resin as well as the bonds between the resin and the carbon fiber are stronger for the panels fabricated by adding GO to the base resin as compared to the panels fabricated by adding pristine graphene to the base resin. The stronger bonds could be due to the better chemical affinity of the GO with the matrix and fibers which well explains why the increase in mechanical properties is more pronounced for the specimens with GO inclusions compared to those with pristine graphene inclusions. Finally, the images also indicates that GO nanoflakes disperse better than pristine graphene in epoxy resin.

Thermal Characterization

Figures 6 and 7 compare the effects of the pristine graphene and GO nanoinclusions on thermal conductivity values of the glass fiber and carbon fiber composites. The base glass fiber and carbon fiber panels had thermal conductivity values of 0.19 and 0.28 W/m K, respectively. Thermal conductivity of the base glass fiber and carbon fiber panels increased to 0.22 and 0.31 W/m .K, respectively, by adding 0.5 wt % of pristine graphene to the resin. Likewise, adding 0.5 wt % GO to the resin improved thermal conductivity of the base glass fiber and carbon fiber panels to 0.23 and 0.33 W/m K.

As shown, the rate of increase in thermal conductivity with respect to the weight percentage of nanoinclusions was reduced for both the glass fiber and carbon fiber panels after the amount of nanoinclusions in the resin exceeded 2 wt %. The observed behavior could be attributed to the agglomeration of nanoinclusions at higher concentrations. This phenomenon is usually expected for both functional and non-functional nanoinclusions in the matrix materials.[34,35] The highest increase in thermal conductivity was observed when 4 wt % nanoinclusion was introduced to the resin. Thermal conductivity of the base carbon fiber panel was improved 45% by adding 4 wt % pristine graphene to the resin. Adding the same amount of GO to the resin, increased the thermal conductivity of the base carbon fiber by 52%. However, the improvement in thermal conductivity was more pronounced for the glass fiber-reinforced composites. For example, thermal conductivity of the glass fiber composites was increased 80% (89%) by adding 4 wt % pristine graphene (GO) to the resin.

A significant increase in thermal conductivity of composites was expected by inclusion of graphene nanoinclusion, due to the

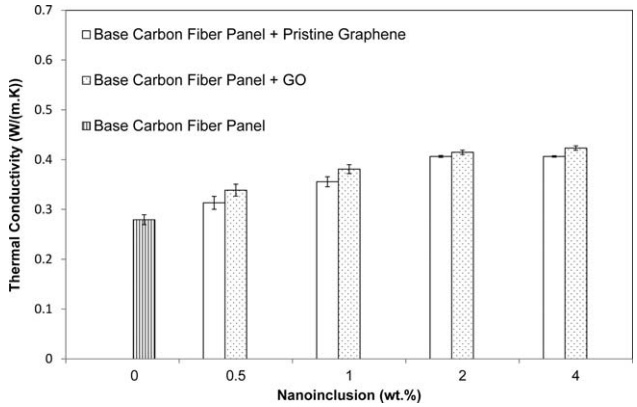

Figure 6. Thermal conductivity of carbon fiber composites for different pristine graphene and GO nanoinclusion.

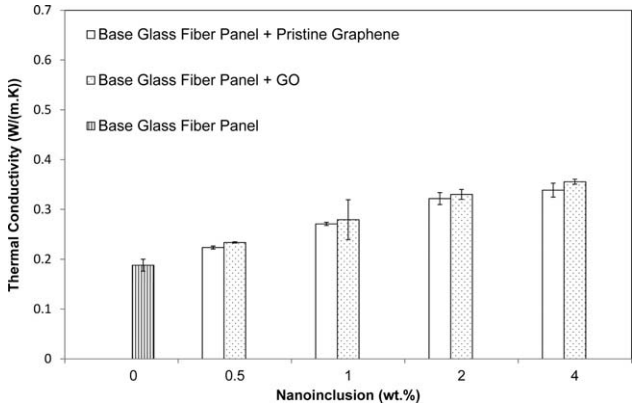

Figure 7. Thermal conductivity of glass fiber composites for different pristine graphene and GO nanoinclusion.

superior thermal conductivity of graphene (around 5000 W/m K). It is notable that the effect of GO on thermal conductivity of the studied panels was more pronounced when compared to the pristine graphene. This suggests that GO created a stronger interfacial bonding between fiber and resin[36] and improved the phonon transfer rate between the two different phases. Superior performance of GO compared to the pristine graphene could also be attributed to the stronger intermolecular forces of GO that allow for a more efficient heat flux and phonon transfer. This observation is in agreement with the findings of Martin-Gallego et al.[37] They reported that the hydroxyl and carbonyl functional groups attached to the edges of CNTs and graphene are the scattering points from which phonons may travel into a polymer system instead of scattering from the crystalline structure of CNTs and graphene when they are in an uncured resin phase. Furthermore, Gojny et al.[38] and Moisala et al.[39] reached similar conclusions for the thermal conductivity of CNTs in the cured-resin phase.

CONCLUSIONS

It was observed that with the inclusions of 0.5–4 wt % graphene (pristine or oxide) in epoxy resin, the physical properties of carbon fiber/epoxy and glass fiber/epoxy composites—called hierarchical graphene composites—improved consistently. It was also observed that the increase in measured mechanical properties was more pronounced for those specimens enhanced with GO, compared to those specimens enhanced with pristine graphene. For example, the compressive strength of glass fiber composites was improved 84% with 4 wt % GO inclusion, while adding the same amount of pristine graphene increased the compressive strength of glass fiber composites 77%. Moreover, inclusion of graphene nanoinclusions consistently increased thermal conductivity of the carbon fiber and glass fiber composites. For instance, the thermal conductivity of glass fiber composites improved 80% and 89% by inclusion of 4 wt % pristine graphene and GO, respectively. The observed improvement in thermal conductivity, similar to the measured mechanical properties, was more for specimens with the GO inclusion than those with the pristine graphene inclusion. This was explained by the fact that the functional groups at the edges of graphene offered stronger molecular bonding, which in turn, resulted in a more efficient heat flux.

Overall, the experimental results reported herein suggest that mechanical and thermal properties of FRPCs, and hence their service life and reliability, can be significantly enhanced by adding pristine graphene or GO nanoinclusions into the epoxy resin system. This means that FRPCs could be a viable replacement for metallic parts in many industries, including wind energy, aerospace, marine, and automotive.

ACKNOWLEDGMENTS

The authors greatly acknowledge the Department of Energy for the financial support (DE- EE0004167) and the National Institute for Aviation Research (NIAR) for the technical support of this work.

REFERENCES

1. Bunsell, A. R.; Renard, J. Fundamentals of Fibre Reinforced Composite Materials; Taylor & Francis Group: Bristol, **2005**.
2. Tong, L.; Mouritz, A. P.; Bannister, M. K. 3D Fibre Reinforced Polymer Composites; Elsevier: Oxford, **2002**.
3. Mall, S.; Rodriguez, J.; Alexander, M. D. *Polym. Compos.* **2011**, *32*, 483.
4. Lubineau, G.; Rahaman, A. *Carbon* **2012**, *50*, 2377.
5. Bortz, D. R.; Merino, C.; Martin-Gullon, I. *Compos. A* **2011**, *42*, 1584.
6. Bekyarova, E.; Thostenson, E. T.; Yu, A.; Kim, H.; Gao, J.; Tang, J.; Hahn, H. T.; Chou, T. W.; Itkis, M. E.; Haddon, R. C. *Langmuir* **2007**, *23*, 3970.
7. Mei, L.; Li, Y.; Wang, R.; Wang, C.; Peng, Q.; He, X. *Polym. Polym. Compos.* **2011**, *19*, 107.
8. Fan, Z.; Santare, M. H.; Advani, S. G. *Compos. A* **2008**, *39*, 540.
9. Qian, H.; Greenhalgh, E. S.; Shaffer, M. S. P.; Bismarck, A. *J. Mater. Chem.* **2010**, *20*, 4751.
10. Tibbetts, G. G.; Lake, M. L.; Strong, K. L.; Rice, B. P. *Compos. Sci. Technol.* **2007**, *67*, 1709.
11. Zhang, Q.; Liu, J.; Sager, R.; Dai, L.; Baur, J. *Compos. Sci. Technol.* **2009**, *69*, 594.
12. Chou, T.-W.; Gao, L.; Thostenson, E. T.; Zhang, Z.; Byun, J.-H. *Compos. Sci. Technol.* **2010**, *70*, 1.
13. Lomov, S. V.; Gorbatikh, L.; Kotanjac, Ž.; Koissin, V.; Houlle, M.; Rochez, O.; Karahan, M.; Mezzo, L.; Verpoest, I. *Compos. Sci. Technol.* **2011**, *71*, 315.
14. Yamamoto, N.; Wicks, S. S.; Guzman De Villoria, R.; Ishiguro, K.; Steiner, S. A., III; Garcia, E. J.; Wardle, B. L. In ICCM International Conferences on Composite Materials, Edinburgh, United Kingdom, **2009**.
15. Qian, H.; Bismarck, A.; Greenhalgh, E. S.; Kalinka, G.; Shaffer, M. S. P. *Chem. Mater.* **2008**, *20*, 1862.
16. Green, K. J.; Dean, D. R.; Vaidya, U. K.; Nyairo, E. *Compos. A* **2009**, *40*, 1470.
17. Novoselov, K. S.; Geim, A. K.; Morozov, S. V.; Jiang, D.; Zhang, Y.; Dubonos, S. V.; Grigorieva, I. V.; Firsov, A. A. *Science* **2004**, *306*, 666.
18. Kuila, T.; Bose, S.; Khanra, P.; Kim, N. H.; Rhee, K. Y.; Lee, J. H. *Compos. A* **2011**, *42*, 1856.
19. Stankovich, S.; Dikin, D. A.; Dommett, G. H. B.; Kohlhaas, K. M.; Zimney, E. J.; Stach, E. A.; Piner, R. D.; Nguyen, S. T.; Ruoff, R. S. *Nature* **2006**, *442*, 282.
20. Ramanathan, T.; Abdala, A. A.; Stankovich, S.; Dikin, D. A.; Herrera Alonso, M.; Piner, R. D.; Adamson, D. H.; Schniepp, H. C.; Chen, X.; Ruoff, R. S.; Nguyen, S. T.; Aksay, I. A.; Prud'Homme, R. K.; Brinson, L. C. *Nat. Nanotechnol.* **2008**, *3*, 327.
21. Yavari, F.; Rafiee, M. A.; Rafiee, J.; Yu, Z. Z.; Koratkar, N. *ACS Appl. Mater. Interfaces* **2010**, *2*, 2738.
22. Asmatulu, R.; Khan, S. I.; Misak, H. In SAMPE Tech Conference, Fort Worth, TX, **2011**.
23. Zhang, X.; Fan, X.; Yan, C.; Li, H.; Zhu, Y.; Li, X.; Yu, L. *ACS Appl. Mater. Interfaces* **2012**, *4*, 1543.
24. Momentive. Technical Data Sheet, 2005. Available at: http://www.momentive.com/Products/TechnicalDataSheet.aspx?id=3937. Accessed on: 3 January **2014**.

25. Park, S.; An, J.; Piner, R. D.; Jung, I.; Yang, D.; Velamakanni, A.; Nguyen, S. T.; Ruoff, R. S. *Chem. Mater.* **2008**, *20*, 6592.

26. Qiu, J.; Zhang, C.; Wang, B.; Liang, R. *Nanotechnology* **2007**, *18*, 275708.

27. Khan, W. S. Ph.D. Dissertation, Department of Mechanical Engineering, Wichita State University, Wichita, KS, **2010**.

28. Khan, W. S.; Asmatulu, R.; Ahmed, I.; Ravigururajan, T. S. *Int. J. Therm. Sci.* **2013**, *71*, 74.

29. Dorigato, A.; Morandi, S.; Pegoretti, A. *J. Compos. Mater.* **2012**, *46*, 1439.

30. Thakre, P. R.; Lagoudas, D. C.; Riddick, J. C.; Gates, T. S.; Frankland, S.-J. V.; Ratcliffe, J. G.; Zhu, J.; Barrera, E. V. *J. Compos. Mater.* **2011**, *45*, 1091.

31. Rahman, M. M.; Hosur, M.; Zainuddin, S.; Jahan, N.; Miller-Smith, E. B.; Jeelani, S. *J. Compos. Mater.* **2014**, in press.

32. Meng, Q. K.; Hetzer, M.; De Kee, D. *J. Compos. Mater.* **2011**, *45*, 1145.

33. Young, R. J.; Kinloch, I. A.; Gong, L.; Novoselov, K. S. *Compos. Sci. Technol.* **2012**, *72*, 1459.

34. Singha, S.; Thomas, M. J. In IEEE Conference on Electrical Insulation and Dielectric Phenomena, Kansas City, MO, **2006**.

35. Allen, E.; Smith, P. *Surfaces* **2001**, *85*, 87.

36. Teng, C.-C.; Ma, C.-C. M.; Chiou, K.-C.; Lee, T.-M. In IMPACT 2010 and International 3D IC Conference, Taipei, Taiwan, **2010**.

37. Martin-Gallego, M.; Verdejo, R.; Khayet, M.; de Zarate, J.; Essalhi, M.; Lopez-Manchado, M. *Nanoscale Res. Lett.* **2011**, *6*, 1.

38. Gojny, F. H.; Wichmann, M. H. G.; Fiedler, B.; Kinloch, I. A.; Bauhofer, W.; Windle, A. H.; Schulte, K. *Polymer* **2006**, *47*, 2036.

39. Moisala, A.; Li, Q.; Kinloch, I. A.; Windle, A. H. *Compos. Sci. Technol.* **2006**, *66*, 1285.